



Heriot-Watt University  
Research Gateway

# Modeling of a combined CH<sub>4</sub>-assisted solid oxide co-electrolysis and Fischer-Tropsch synthesis system for low-carbon fuel production

## Citation for published version:

Xu, H, Maroto-Valer, MM, Ni, M, Cao, J & Xuan, J 2019, 'Modeling of a combined CH<sub>4</sub>-assisted solid oxide co-electrolysis and Fischer-Tropsch synthesis system for low-carbon fuel production', *Energy Procedia*, vol. 158, pp. 1666-1671. <https://doi.org/10.1016/j.egypro.2019.01.388>

## Digital Object Identifier (DOI):

[10.1016/j.egypro.2019.01.388](https://doi.org/10.1016/j.egypro.2019.01.388)

## Link:

[Link to publication record in Heriot-Watt Research Portal](#)

## Document Version:

Publisher's PDF, also known as Version of record

## Published In:

Energy Procedia

## General rights

Copyright for the publications made accessible via Heriot-Watt Research Portal is retained by the author(s) and / or other copyright owners and it is a condition of accessing these publications that users recognise and abide by the legal requirements associated with these rights.

## Take down policy

Heriot-Watt University has made every reasonable effort to ensure that the content in Heriot-Watt Research Portal complies with UK legislation. If you believe that the public display of this file breaches copyright please contact [open.access@hw.ac.uk](mailto:open.access@hw.ac.uk) providing details, and we will remove access to the work immediately and investigate your claim.



10<sup>th</sup> International Conference on Applied Energy (ICAE2018), 22-25 August 2018, Hong Kong, China

## Modeling of a combined CH<sub>4</sub>-assisted solid oxide co-electrolysis and Fischer-Tropsch synthesis system for low-carbon fuel production

Haoran Xu<sup>a</sup>, M. Mercedes Maroto-Valer<sup>a,\*</sup>, Meng Ni<sup>b</sup>, Jun Cao<sup>c</sup>, Jin Xuan<sup>d,\*</sup>

<sup>a</sup>Research Centre for Carbon Solutions (RCCS), School of Engineering & Physical Sciences, Heriot-Watt University, Edinburgh, EH14 4AS, United Kingdom

<sup>b</sup>Building Energy Research Group, Department of Building and Real Estate, The Hong Kong Polytechnic University, Hung Hom, Kowloon, Hong Kong, China

<sup>c</sup>State Key Laboratory of Chemical Engineering, School of Mechanical and Power Engineering, East China University of Science and Technology, Shanghai, China

<sup>d</sup>Department of Chemical Engineering, Loughborough University, Loughborough, United Kingdom

### Abstract

CH<sub>4</sub>-assisted solid oxide electrolyzer cells (SOECs) can co-electrolyze H<sub>2</sub>O and CO<sub>2</sub> effectively for simultaneous energy storage and CO<sub>2</sub> utilization. Compared with conventional SOECs, CH<sub>4</sub>-assisted SOECs consume less electricity because CH<sub>4</sub> in the anode provides part of the energy for electrolysis. As syngas (CO and H<sub>2</sub> mixture) is generated from the co-electrolysis process, it is necessary to study its utilization through the subsequent processes, such as Fischer-Tropsch (F-T) synthesis. An F-T reactor can convert syngas into hydrocarbons, and thus it is very suitable for the utilization of syngas. In this paper, the combined CH<sub>4</sub>-assisted SOEC and F-T synthesis system is numerically studied. Validated 2D models for CH<sub>4</sub>-assisted SOEC and F-T processes are adopted for parametric studies. It is found that the cathode inlet H<sub>2</sub>O/CO<sub>2</sub> ratio in the SOEC significantly affects the production components through the F-T process. Other operating parameters such as the operating temperature and applied voltage of the SOEC are found to greatly affect the productions of the system. This model can be used for understanding and design optimization of the combined fuel-assisted SOEC and F-T synthesis system to achieve economical hydrocarbon generation.

© 2019 The Authors. Published by Elsevier Ltd.

This is an open access article under the CC BY-NC-ND license (<http://creativecommons.org/licenses/by-nc-nd/4.0/>)

Peer-review under responsibility of the scientific committee of ICAE2018 – The 10th International Conference on Applied Energy.

**Keywords:** Solid oxide electrolyzer cell; Fischer-Tropsch synthesis; Mathematical modeling; Hydrocarbon generation

\* Corresponding authors. Tel.: +44 (0)131 451 3293; fax: +44 (0)131 451 3293.

E-mail address: [m.maroto-valer@hw.ac.uk](mailto:m.maroto-valer@hw.ac.uk) (MMV); [j.xuan@lboro.ac.uk](mailto:j.xuan@lboro.ac.uk) (JX)

## 1. Introduction

With the growing attention on global warming, effective CO<sub>2</sub> utilization methods are urgently needed. Solid oxide electrolyzer cells (SOECs) are promising technologies to convert CO<sub>2</sub> into chemical fuels such as CO. Compared with low-temperature electrolyzers, SOECs consume less electrical energy as part of the input energy comes from heat. The high operating temperature also allows the use of non-noble catalysts in the SOEC, leading to a lower overall cost. Recently, the concept of fuel-assisted SOECs has been demonstrated, where low-cost fuels (e.g. methane) are supplied to the anode to reduce the operating potentials of the SOEC [1]. The fuel-assisted SOECs can even electrolyze oxidants without consuming electricity, which means it is possible to convert CO<sub>2</sub> to fuels by only consuming low-cost fuels in the SOEC [2].

SOECs can co-electrolyze H<sub>2</sub>O and CO<sub>2</sub> and generate syngas (H<sub>2</sub> and CO mixture), which can be further utilized in the Fischer-Tropsch (F-T) reactor for low carbon fuel production [3, 4]. As methane is usually less wanted from the F-T synthesis process, it is therefore suitable to use methane as the assistant fuel in the SOEC for CO<sub>2</sub> and H<sub>2</sub>O co-electrolysis. A system consisting of a CH<sub>4</sub>-assisted SOEC and a F-T reactor is very promising for CO<sub>2</sub> utilization and hydrocarbon fuel generation. However, despite some preliminary studies on the combined SOEC and F-T systems [5, 6], no study on a combined fuel-assisted SOEC and F-T reactor system has been conducted thus far. To fill this research gap, in this work 2D mathematical models are developed for a combined CH<sub>4</sub>-assisted SOEC and F-T reactor system for H<sub>2</sub>O/CO<sub>2</sub> co-electrolysis and hydrocarbon fuel generation. The sub-models for the CH<sub>4</sub>-assisted SOEC and the F-T reactor are validated in the previous studies [7, 8]. Parametric simulations are conducted to understand the characteristics of such a system and the interplay of different physical/chemical processes.

## 2. Model description

The proposed hybrid system consists of a CH<sub>4</sub>-assisted SOEC and a F-T reactor, as shown in Fig. 1. In the SOEC anode, CH<sub>4</sub> and H<sub>2</sub>O are supplied to anode with a ratio of 1:1.5 to avoid methane coking. CO<sub>2</sub> and H<sub>2</sub>O are supplied to the cathode, where they are electrolyzed to generate syngas. Syngas generated from the SOEC section is collected for F-T reactor, where hydrocarbons are generated through the synthesis process.

2D numerical models are developed to simulate the characteristics of the system, the model kinetics for both the CH<sub>4</sub>-assisted SOEC and the F-T reactor are validated by using prior published work [7, 8]. The tubular SOEC has a length of 7 cm, an inner diameter of 0.3 cm and an outer diameter of 0.5 cm. It uses Ni-YSZ as anode support layer, Ni-ScSZ as anode active layer, ScSZ as electrolyte and Ni-ScSZ as cathode. The tubular F-T reactor has a length of 30 cm and an outer diameter of 1 cm. It uses Fe based catalyst for the improvement of synthesis reaction rates. The material properties for the SOEC can be found in Table 1.

For model simplification, the following assumptions are adopted:

1. The electrochemical reaction active sites are assumed to be uniformly distributed in the porous electrodes.
2. The electronic and ionic conducting phases are continuous and homogeneous in the porous electrodes.
3. All the gases are considered as ideal gases.
4. Temperature distribution is uniform in the reactors due to the small size.

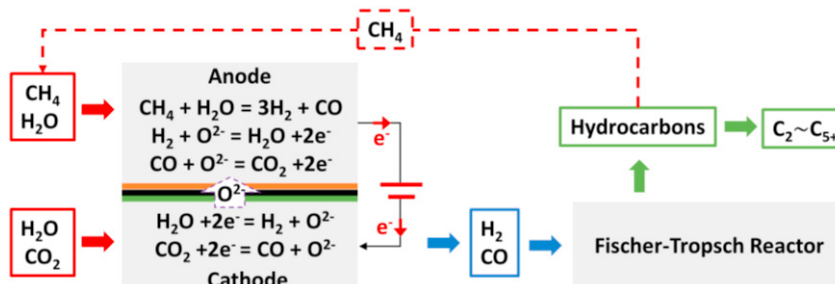


Fig. 1. Schematic of combined CH<sub>4</sub>-assisted SOEC and F-T reactor system

Table 1. Material properties.

| Parameters      | Value or expression                 | Unit       |
|-----------------|-------------------------------------|------------|
| $\sigma_{ScSZ}$ | $69200 \times e^{\frac{-9681}{T}}$  | $S m^{-1}$ |
| $\sigma_{YSZ}$  | $33400 \times e^{\frac{-10300}{T}}$ | $S m^{-1}$ |
| $\sigma_{Ni}$   | $4.2 \times 10^6 - 1065.3T$         | $S m^{-1}$ |
| $\epsilon$      | 0.36                                |            |
| $\tau$          | 3                                   |            |
| $S_{TPB}$       | $2.14 \times 10^5$                  | $m^{-1}$   |

### 2.1. Sub-model of $CH_4$ -assisted SOEC for $CO_2$ and $H_2O$ co-electrolysis

As shown in Fig. 1, the gas mixture of  $H_2O$  and  $CO_2$  flows into the cathode channel, while the gas mixture of  $CH_4$ , and  $H_2O$  flows into the anode channel. In the cathode, both  $H_2O$  and  $CO_2$  are reduced to generate  $H_2$  and  $CO$  as shown in Eq. (1) and Eq. (2), respectively.



In the anode, the methane steam reforming (MSR) reaction happens to generate  $H_2$  and  $CO$ , which are then electrochemically oxidized by the  $O^{2-}$  transported from the cathode. The MSR reaction and electrochemical oxidizations of  $H_2$  and  $CO$  are listed as shown in Eq. (3) to Eq. (5).



Due to the existence of  $H_2O$  and  $CO$ , water gas shift reaction (WGSR) occurs in both anode and cathode as



In operation, the required voltage applied to SOEC can be calculated by Eq. (7):

$$V = E + \eta_{act} + \eta_{ohmic} \quad (7)$$

where  $E$  is the equilibrium potential related with thermodynamics;  $\eta_{act}$  is the activation overpotentials reflecting the electrochemical activities and  $\eta_{ohmic}$  is the ohmic overpotential calculated by the Ohmic law.

The calculation of equilibrium potential is based on oxygen partial pressure [9] and calculated as:

$$E = \frac{RT}{nF} \ln \left( \frac{\sum P_{O_2,ca}^L}{\sum P_{O_2,an}^L} \right) \quad (8)$$

where  $R$  is the universal gas constant ( $8.3145 J mol^{-1} K^{-1}$ ),  $T$  is temperature (K),  $F$  is the Faraday constant ( $96485 C mol^{-1}$ ),  $n$  is the number of electrodes transferred per electrochemical reaction,  $P_{O_2,ca}^L$  and  $P_{O_2,an}^L$  are oxygen partial pressures in the cathode and anode, respectively.

For the pairs of  $H_2O/H_2$  and  $CO_2/CO$ , their oxygen partial pressures can be expressed by:

$$P_{O_2,(H_2O/H_2)}^L = \left( \frac{P_{H_2O}^L}{P_{H_2}^L} \cdot e^{\frac{\Delta G_{H_2O/H_2}}{RT}} \right)^2, \text{ and} \quad (9)$$

$$P_{O_2,(CO_2/CO)}^L = \left( \frac{P_{CO_2}^L}{P_{CO}^L} \cdot e^{\frac{\Delta G_{CO_2/CO}}{RT}} \right)^2, \quad (10)$$

where  $P_{H_2O}^L$ ,  $P_{H_2}^L$ ,  $P_{CO_2}^L$  and  $P_{CO}^L$  are local partial pressures of  $H_2O$ ,  $H_2$ ,  $CO_2$  and  $CO$ , respectively.  $\Delta G_{H_2O/H_2}$  and  $\Delta G_{CO_2/CO}$  are the Gibbs free energy change in the  $H_2$  and  $CO$  oxidation reactions, respectively.

The activation overpotential is calculated by the Butler-Volmer equation

$$i = i_0 \left\{ \exp \left( \frac{\alpha n F \eta_{act}}{RT} \right) - \exp \left( \frac{-(1-\alpha) n F \eta_{act}}{RT} \right) \right\} \quad (11)$$

where  $i_0$  is the exchange current density and  $\alpha$  is the electronic transfer coefficient. For  $H_2O$  electrolysis, the exchange current density can be further expressed as

$$i_0 = \beta \frac{P_{H_2O}}{P_{ref}} \frac{P_{H_2}}{P_{ref}} \exp \left( -\frac{E_a}{RT} \right) \quad (12)$$

where  $\beta$  is the activity factor and  $E_a$  is the activation energy. For  $\text{CO}_2$  electrolysis, its exchange current density is 0.45 times of  $\text{H}_2\text{O}$  electrolysis [10]. All the kinetics for above reactions can be found in Table 2.

Table 2. Reaction kinetic parameters

| Parameters                    | Value or expression  | Unit   |
|-------------------------------|--|--|
| $\beta$                       | $3.3 \times 10^8$  | $\text{Am}^{-2}$                                 |
| $E_a$                         | $1.2 \times 10^5$  | $\text{J mol}^{-1}$                              |
| $\alpha_{\text{H}_2\text{O}}$ | 0.65   |  |
| $\alpha_{\text{CO}_2}$        | 0.65   |  |
| $R_{\text{MSR}}$ [11]         | $k_{\text{rf}}(p_{\text{CH}_4} p_{\text{H}_2\text{O}} - \frac{p_{\text{H}_2} p_{\text{CO}}}{K_{\text{pr}}})$ | $\text{mol m}^{-3} \text{s}^{-1}$                |
| $k_{\text{rf}}$               | $2395 \exp(\frac{-231266}{RT})$  | $\text{mol m}^{-3} \text{Pa}^{-2} \text{s}^{-1}$ |
| $K_{\text{pr}}$               | $1.0267 \times 10^{10} \exp(-0.2513Z^4 + 0.3665Z^3 + 0.5810Z^2 - 27.134Z + 3.277)$                           |  |
| $R_{\text{WGSR}}$ [12]        | $k_{\text{sf}}(p_{\text{H}_2\text{O}} p_{\text{CO}} - \frac{p_{\text{H}_2} p_{\text{CO}_2}}{K_{\text{ps}}})$ | $\text{mol m}^{-3} \text{s}^{-1}$                |
| $k_{\text{sf}}$               | $0.0171 \exp(\frac{-103191}{RT})$  | $\text{mol m}^{-3} \text{Pa}^{-2} \text{s}^{-1}$ |
| $K_{\text{ps}}$               | $\exp(-0.2935Z^3 + 0.6351Z^2 + 4.1788Z + 0.3169)$  |  |
| $Z$                           | $\frac{1000}{T} - 1$   |  |

## 2.2. Sub-model of F-T reactor

The F-T reactor uses Fe-HZSM5 as catalyst and works at 573 K and 2 MPa for syngas synthesis. The reactions in the F-T process are shown in Eq. (13) to Eq. (20).



The reaction kinetics for above reactions can be expressed as [8]

$$R_i = 0.278k_i \exp(-\frac{E_i}{RT}) p_{\text{CO}}^m \cdot p_{\text{H}_2}^n, \quad (21)$$

## 2.3. CFD Sub-model

For both the SOEC and the F-T reactor, the mass transport of gas species is calculated by extended Fick's law

$$N_i = -\frac{1}{RT} \left( \frac{B_0 y_i P}{\mu} \nabla P - D_i^{\text{eff}} \nabla (y_i P) \right) \quad (i = 1, \dots, n), \quad (22)$$

where  $B_0$  is the material permeability,  $\mu$  is the gas viscosity,  $y_i$  and  $D_i^{\text{eff}}$  are the mole fraction and effective diffusion coefficient of component  $i$ , respectively.  $D_i^{\text{eff}}$  can be further determined by

$$D_i^{\text{eff}} = \frac{\varepsilon}{\tau} \left( \frac{1}{D_{\text{im}}^{\text{eff}}} + \frac{1}{D_{\text{ik}}^{\text{eff}}} \right)^{-1}, \quad (23)$$

where  $\varepsilon$  is the porosity,  $\tau$  is the tortuosity factor,  $D_{\text{im}}^{\text{eff}}$  is the molecular diffusion coefficient and  $D_{\text{ik}}^{\text{eff}}$  is the Knudsen diffusion coefficient [13].

The mass conservation can be described by

$$\nabla(-D_i^{\text{eff}} \nabla c_i) = r_i, \quad (24)$$

where  $c_i$  is the gas molar concentration and  $r_i$  is the mass source term of the gaseous species.

Navier-Stokes equation with Darcy's term is adopted to calculate the momentum transport in both the SOEC and F-T reactor as shown in Eq. (25).

$$\rho \frac{\partial \mathbf{u}}{\partial t} + \rho \mathbf{u} \nabla \mathbf{u} = -\nabla p + \nabla [\mu (\nabla \mathbf{u} + (\nabla \mathbf{u})^T) - \frac{2}{3} \mu \nabla \mathbf{u}] - \frac{\varepsilon \mu \mathbf{u}}{k} \quad (25)$$

Here  $\rho$  is the gas density and  $\mathbf{u}$  is the velocity vector.

#### 2.4. Boundary conditions and model solution

Electric potentials are specified at the outer surface of two electrodes with the cell ends electrical insulated. Inlet gas flow rate and mole fraction of the species are given at inlets of the SOEC. The ratio of  $\text{H}_2$  to  $\text{CO}$  for F-T reactor inlet is consistent with the ratio of  $\text{H}_2$  to  $\text{CO}$  of SOEC cathode outlet. The numerical models are solved at given parameters using commercial software COMSOL MULTIPHYSICS<sup>®</sup>.

### 3. Results and discussions

As shown in Fig. 2(a), with the increase of SOEC operating temperature, the mole fractions of  $\text{H}_2$  and  $\text{CO}$  in the outlets significantly increase due to the improved electrochemical activity. With the more complete conversion of  $\text{CO}_2$  at higher temperatures, the ratio of outlet  $\text{H}_2/\text{CO}$  continuously decreases from  $\sim 8$  to  $\sim 1$ , indicating the much-increased  $\text{CO}$  fraction in the generated syngas.

Besides, the applied voltage largely affects the performance of the SOEC, as shown in Fig. 2(b). Compared with traditional SOECs working at 1V  $\sim$  3 V applied voltage, the  $\text{CH}_4$ -assisted SOEC performs well at a low applied voltage. The mole fraction of syngas in the outlet is closed to 1 at 0.7 V and the cell can even work at 0 V applied voltage with the driven force provided by  $\text{CH}_4$  in the anode, which means no input electrical power is needed. Therefore, the SOEC offers a high conversion rate while only consume very limited electricity benefited from methane assistance.

The characteristic of  $\text{C}_n\text{H}_m$  production with the change of inlet  $\text{H}_2/\text{CO}$  ratio from the F-T reactor is shown in Fig. 2(c), where the mole fraction of both total hydrocarbons and  $\text{CH}_4$  are found to be improved with the increase of inlet  $\text{H}_2$  mole fraction. For comparison, the outlet mole fractions of  $\text{C}_2\text{H}_6$ ,  $\text{C}_3\text{H}_8$  and  $\text{C}_{5+}$  show slightly increase at higher inlet  $\text{H}_2$  mole fraction, while nearly no changed is found on the outlet mole fractions of  $\text{C}_2\text{H}_4$  and  $\text{C}_4\text{H}_{10}$ .

Finally, the mole fractions of low-carbon fuels production from the F-T reactor with the change of inlet  $\text{H}_2\text{O}/\text{CO}_2$  ratio of the  $\text{CH}_4$ -assisted SOEC is shown in Fig. 2(d). At small  $\text{H}_2\text{O}/\text{CO}_2$  ratio (0.3: 0.7) for SOEC inlet, the F-T reactor generates 4 times  $\text{C}_2 \sim \text{C}_{5+}$  as much as  $\text{CH}_4$ . When the  $\text{H}_2\text{O}/\text{CO}_2$  ratio increases 0.5: 0.5, the outlet  $\text{C}_2 \sim \text{C}_{5+}$  and  $\text{CH}_4$  also comes to a similar level. At the 0.6: 0.4  $\text{H}_2\text{O}/\text{CO}_2$  ratio,  $\text{CH}_4$  generated by the F-T reactor becomes much larger than  $\text{C}_2 \sim \text{C}_{5+}$  with a ratio close to 2: 1.

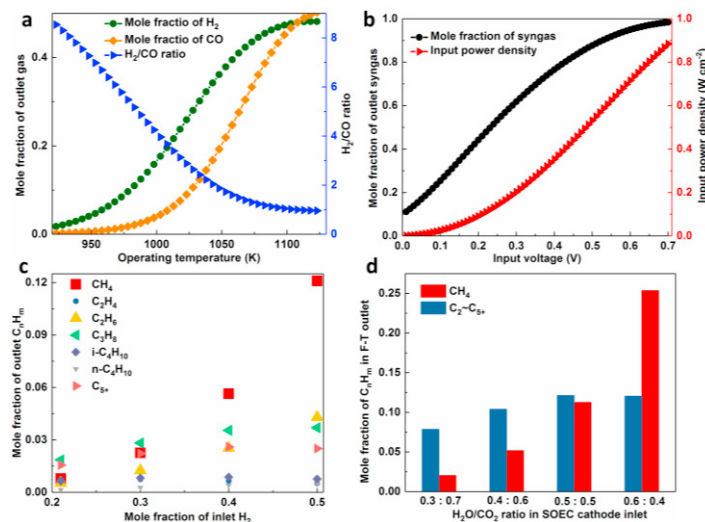


Fig. 2. (a, b) The effects of SOEC operating parameters on its performance; (c) the effects of F-T reactor inlet H<sub>2</sub>/CO ratio on its outlet hydrocarbon components; (d) the effect of SOEC inlet H<sub>2</sub>O/CO<sub>2</sub> ratio on the outlet hydrocarbon components of the F-T reactor.

#### 4. Conclusions

The first 2D model combining a CH<sub>4</sub>-assisted solid oxide co-electrolysis and Fischer-Tropsch synthesis system for low-carbon fuel production is developed in this paper. The kinetics of the model are validated by using previous studies. CO<sub>2</sub> and H<sub>2</sub>O are used as the raw materials in the SOEC section for the generation of low-carbon fuel through the F-T reactor. By conducting parametric studies, it is found that the operating temperature, the applied voltage and the inlet H<sub>2</sub>O/CO<sub>2</sub> ratio significantly affect the outlet syngas components of SOEC, thus greatly affect the characteristics of the hydrocarbons synthesized by the F-T reactor. As a result, the mole fractions of CH<sub>4</sub> and C<sub>2</sub> ~ C<sub>5+</sub> generated by the F-T reactor can be controlled by adjusting the inlet H<sub>2</sub>O/CO<sub>2</sub> ratio in the electrolysis process. This study builds a solid foundation for the understanding and optimization of a combined fuel-assisted SOEC and F-T reactor system.

#### Acknowledgements

The research is supported by the UK Engineering and Physical Science Research Council (EPSRC) through grants EP/K021796/1 and EP/N009924/1.

#### References

- [1] Luo Y, Shi Y, Li W, Ni M, Cai N. Elementary reaction modeling and experimental characterization of solid oxide fuel-assisted steam electrolysis cells. *International Journal of Hydrogen Energy*. 2014;39:10359-73.
- [2] Xu H, Chen B, Ni M. Modeling of Direct Carbon-Assisted Solid Oxide Electrolysis Cell (SOEC) for Syngas Production at Two Different Electrodes. *J Electrochem Soc*. 2016;163:F3029-F35.
- [3] Chen L, Chen F, Xia C. Direct synthesis of methane from CO<sub>2</sub>-H<sub>2</sub>O co-electrolysis in tubular solid oxide electrolysis cells. *Energy & Environmental Science*. 2014;7:4018-22.
- [4] Chen B, Xu H, Chen L, Li Y, Xia C, Ni M. Modelling of One-Step Methanation Process Combining SOECs and Fischer-Tropsch-like Reactor. *J Electrochem Soc*. 2016;163:F3001-F8.
- [5] Becker WL, Braun RJ, Penev M, Melaina M. Production of Fischer-Tropsch liquid fuels from high temperature solid oxide co-electrolysis units. *Energy*. 2012;47:99-115.
- [6] Stempien JP, Ni M, Sun Q, Chan SH. Thermodynamic analysis of combined Solid Oxide Electrolyzer and Fischer-Tropsch processes. *Energy*. 2015;81:682-90.
- [7] Xu H, Chen B, Irvine J, Ni M. Modeling of CH<sub>4</sub>-assisted SOEC for H<sub>2</sub>O/CO<sub>2</sub> co-electrolysis. *International Journal of Hydrogen Energy*. 2016;41:21839-49.
- [8] Rahimpour MR, Elekaei H. A comparative study of combination of Fischer-Tropsch synthesis reactors with hydrogen-permselective membrane in GTL technology. *Fuel Processing Technology*. 2009;90:747-61.
- [9] Stempien JP, Liu Q, Ni M, Sun Q, Chan SH. Physical principles for the calculation of equilibrium potential for co-electrolysis of steam and carbon dioxide in a Solid Oxide Electrolyzer Cell (SOEC). *Electrochimica Acta*. 2014;147:490-7.
- [10] Luo Y, Shi Y, Li W, Cai N. Comprehensive modeling of tubular solid oxide electrolysis cell for co-electrolysis of steam and carbon dioxide. *Energy*. 2014;70:420-34.
- [11] Ni M. 2D heat and mass transfer modeling of methane steam reforming for hydrogen production in a compact reformer. *Energy Conversion and Management*. 2013;65:155-63.
- [12] Ni M. An electrochemical model for syngas production by co-electrolysis of H<sub>2</sub>O and CO<sub>2</sub>. *Journal of Power Sources*. 2012;202:209-16.
- [13] Suwanwarangkul R, Croiset E, Fowler MW, Douglas PL, Entchev E, Douglas MA. Performance comparison of Fick's, dusty-gas and Stefan-Maxwell models to predict the concentration overpotential of a SOFC anode. *Journal of Power Sources*. 2003;122:9-18.